SCIENTIFIC REPORTS

OPEN

SUBJECT AREAS:
CELL DEATH IN THE NERVOUS SYSTEM
INFLAMMASOME

Received
4 February 2014

Accepted
18 March 2014

Published
3 April 2014

Correspondence and requests for materials should be addressed to G.D. (gdahl@miami.edu)

ATP and potassium ions: a deadly combination for astrocytes

David G. Jackson[1], Junjie Wang[1], Robert W. Keane[1], Eliana Scemes[2] & Gerhard Dahl[1]

[1]Department of Physiology and Biophysics, University of Miami School of Medicine, Miami, Florida 33136, [2]Dominick P. Purpura Department of Neuroscience, Albert Einstein College of Medicine, Bronx, New York, 10461.

The ATP release channel Pannexin1 (Panx1) is self-regulated, i.e. the permeant ATP inhibits the channel from the extracellular space. The affinity of the ATP binding site is lower than that of the purinergic $P2X_7$ receptor allowing a transient activation of Panx1 by ATP through $P2X_7R$. Here we show that the inhibition of Panx1 by ATP is abrogated by increased extracellular potassium ion concentration ($[K^+]_o$) in a dose-dependent manner. Since increased $[K^+]_o$ is also a stimulus for Panx1 channels, it can be expected that a combination of ATP and increased $[K^+]_o$ would be deadly for cells. Indeed, astrocytes did not survive exposure to these combined stimuli. The death mechanism, although involving $P2X_7R$, does not appear to strictly follow a pyroptotic pathway. Instead, caspase-3 was activated, a process inhibited by Panx1 inhibitors. These data suggest that Panx1 plays an early role in the cell death signaling pathway involving ATP and K^+ ions. Additionally, Panx1 may play a second role once cells are committed to apoptosis, since Panx1 is also a substrate of caspase-3.

ATP- induced cell death is a well-established consequence of overstimulation of the innate immune response[1–4]. This form of cellular demise is mainly mediated by the ionotropic purinergic receptors $P2X_7$ and $P2X_4$ interacting with the inflammasome[5–7]. In this context, ATP is involved in secondary cell death subsequent to the initial lesions in CNS injury or stroke. Cells damaged by the initial insult release ATP together with a host of other compounds including glutamate and potassium ions. Due to the limited extracellular space in the CNS, the efflux of these compounds results in accumulation to concentrations sufficiently high to activate the low affinity receptors such as $P2X_7$ by ATP, for example. Furthermore, efflux of potassium ions can elevate the concentration of K^+ in the extracellular space to values as high as 60 mM[8–10], a condition known to activate Panx1 channels[7,11].

There is evidence that Panx1 plays a critical role in ATP-mediated cell death[7,12]. Panx1 channel activity can be initiated by ATP binding to purinergic receptors, including the $P2X_7$ receptor[13,14]. Open Panx1 channels are permeable to ATP and thus an ATP-induced ATP release ensues[15]. In theory, even small amounts of extracellular ATP could trigger cell death based on this positive feedback loop. However, such profligate cell death typically is not encountered in response to purinergic receptor activation indicating the presence of counteractive measures to hyperactivation of the innate immune response. Indeed, such a counteractive mechanism is a component of the ATP release channel itself. Panx1 channels are inhibited by extracellular ATP[16,17]. Thus, a negative feedback loop counteracts the potential overstimulation through the positive feedback between the purinergic receptor and Panx1. The affinity of the binding site on Panx1[18] is lower than that on the $P2X_7$ receptor, allowing a transient amplification of the ATP signal without inducing cell death.

However, there are alternative activation mechanisms for Panx1, including mechanical stress, low oxygen, glutamate through NMDA receptors, and elevation of extracellular potassium ion concentration[7,15,19–22]. In secondary cell death, all these stimulatory factors for Panx1 come together due to their release from damaged cells or in the case of low oxygen due to the consequences of injury or stroke on blood perfusion. The question thus arises whether the combination of stimulatory factors overwhelms the inhibitory pathways and thus cause secondary cell death.

Here we tested the interplay between stimulatory and inhibitory factors on the Panx1 channel in mediating cell death. Specifically, we analyzed whether stimulation of the Panx1 channel by K^+ or its inhibition by ATP predominate in controlling channel function.

Results

Extracellular K^+ attenuates the inhibition of Panx1 channels by ATP and its analogue, BzATP. Panx1 channels can be activated by stepping the membrane potential to positive potentials or maintaining it there.

Although such membrane potentials are unlikely to occur *in vivo* except at the brief peak of action potentials, activation by voltage is an experimentally convenient way to elicit and observe Panx1 channel activity. Figure 1a shows Panx1 channel currents induced by a voltage step protocol. Application of ATP or BzATP to the bath reversibly inhibited the Panx1 currents as described previously[16–18]. The ATP analogue BzATP, exerted the same effect as ATP, however, requiring lower concentrations. Also, as shown previously[7], increasing the extracellular K^+ concentration resulted in Panx1 currents even when the membrane potential was clamped at the resting membrane potential (−50 mV). However, when ATP or BzATP were applied to the K^+-activated Panx1 channel, current inhibition by ATP at a concentration of 500 μM or BzATP at 30 μM (Figure 1a) or 300 μM (Figure 1 b) was attenuated. This attenuation was dependent on the K^+ concentration used as Panx1 stimulus. At 75 mM extracellular $[K^+]$, even 300 μM BzATP remained ineffective, while probenecid inhibited the K^+-induced current (Fig. 1c). The same pulse protocol applied to uninjected control oocytes elicited small currents, which were not inhibited by 300 μM BzATP. Similarly, K^+ induced a small current of unknown origin, which was not inhibited by BzATP (Figure 1d).

The normally low extracellular K^+ concentration did not interfere with the inhibitory effect of ATP on Panx1 currents. Only when the K^+ concentration was increased to 10 mM was an attenuation of the ATP inhibition discernible. The effect of K^+ was dose dependent and saturated at 75 mM $[K^+]_o$ (Figure 2a). These findings indicate, that the effect of BzATP on Panx1 currents can be overcome by increasing $[K^+]_o$.

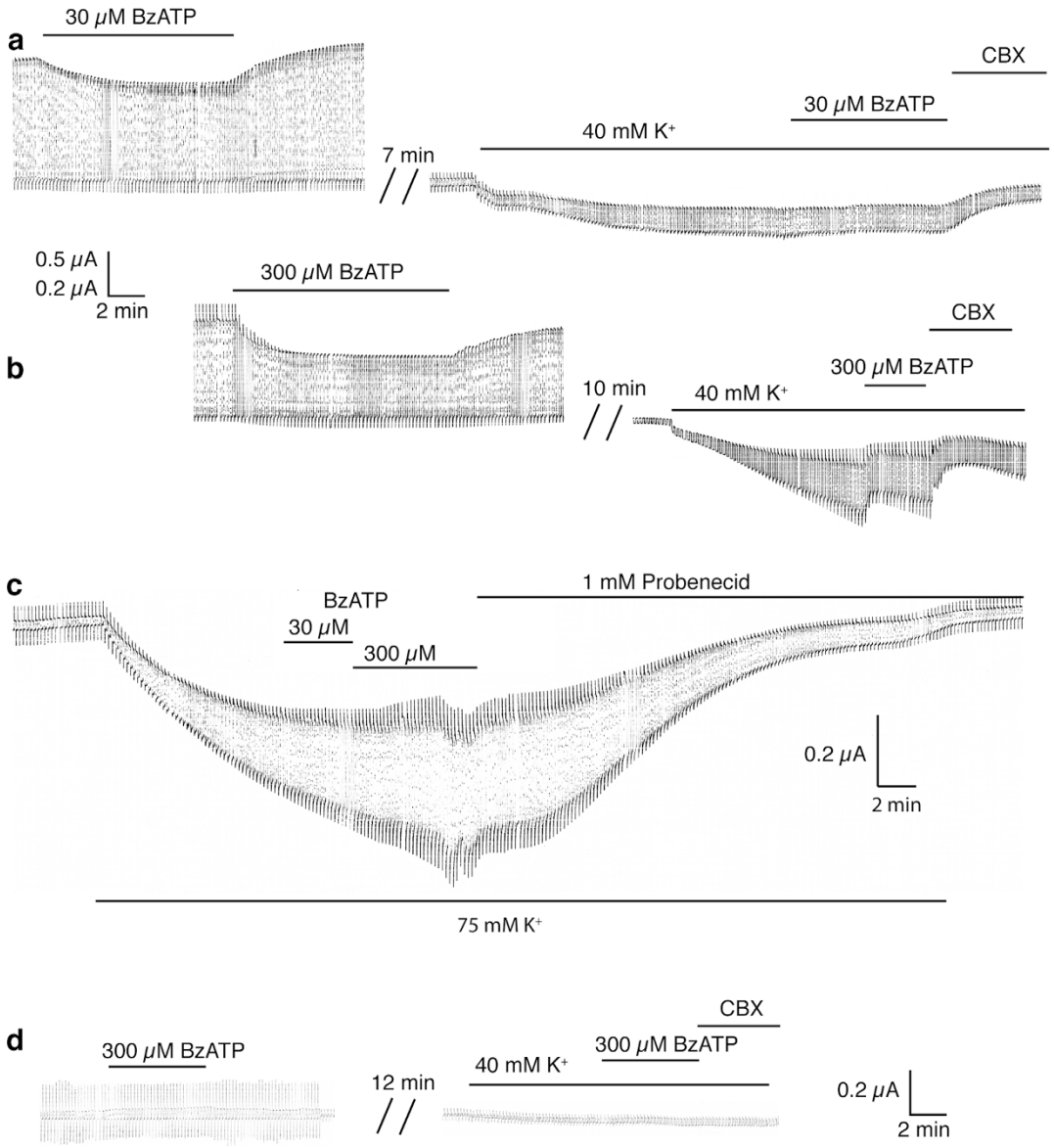

Figure 1 | Extracellular K^+ attenuates the inhibitory effect of BzATP on Panx1 channel currents in *Xenopus* oocytes. (a) BzATP (30 μM) applied to oocytes expressing Panx1 and repeatedly pulsed from a holding potential of −60 mV to +60 mV to open the channels significantly attenuated the currents. Application of 40 mM $[K^+]_o$ to the same cell held at −50 mV and pulsed to −40 mV induced an inward current, indicating opening of Panx1 channels. The currents were slightly affected by 30 μM BzATP but were diminished by 100 μM carbenoxolone (CBX). (b) At 300 μM, BzATP inhibited both voltage- and K^+-induced currents. (c) With 75 mM $[K^+]$ as stimulus, neither 30 nor 300 μM BzATP had a discernible inhibitory effect. (d) In uninjected control oocytes, the pulse protocol induced small currents that were not inhibited by 300 μM BzATP. As reported earlier[7], increased extracellular K^+ (40 mM) induced a small current of unknown origin in these cells. This K^+-induced current was also not affected by BzATP (300 μM).

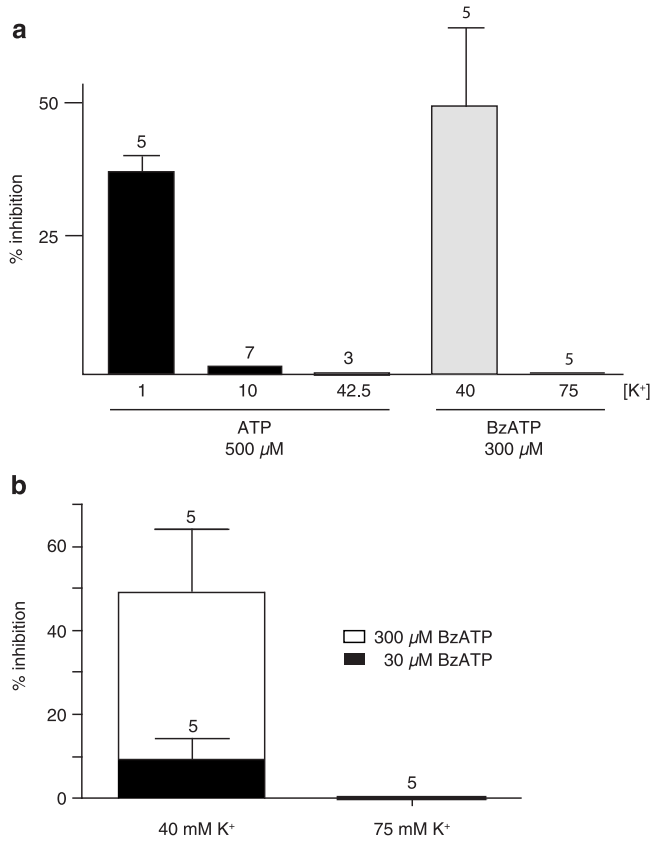

Figure 2 | Quantitative analysis of inhibition of Panx1 currents by ATP or BzATP at different K^+ concentrations. (a) In normal Ringer solution (1 mM K^+), 500 μM ATP inhibited voltage-induced currents. With the same ATP concentration, currents induced by K^+ were minimally affected (10 mM $[K^+]_o$) or not at all (42.5 mM $[K^+]_o$). BzATP (300 μM) was effectively inhibiting at 40 mM $[K^+]_o$, but not at 75 mM. (b) Competition between BzATP and K^+. At 40 mM $[K^+]_o$, increasing the BzATP concentration restored the inhibitory capacity of this compound. Increasing the $[K^+]_o$ to 75 mM eliminated the inhibitory effect of even 300 μM BzATP.

Do ATP and K^+ compete at an extracellular binding site? ATP inhibits Panx1 from the extracellular side involving amino acids in both extracellular loops of the protein[18]. Activation of Panx1 by K^+ is initiated also at the extracellular surface and is dose-dependent starting at 10 mM $[K^+]_o$[7,11]. To test whether ATP and K^+ act on similar segments of the extracellular portions of Panx1, different ATP/BzATP concentrations were applied at constant $[K^+]_o$. As shown in Figure 2b, by increasing the BzATP concentration, the attenuation of inhibition by K^+ was in part overcome at $[K^+]_o$ up to 40 mM. Only at $[K^+]_o$ of 75 mM increasing [BzATP] to 300 μM did not restore inhibition of the currents anymore. These data are consistent with competition between ATP and K^+ at a common (at least in part overlaping) binding site.

Effect of K^+ on other Panx1 inhibitors. To test whether K^+ interferes with general gating mechanisms of the Panx1 channel, the inhibitory action of a series of Panx1 blockers[16,23–26]; was tested. As shown in Figure 3, the effects of probenecid, BBG and carbenoxolone on Panx1 currents was independent of the presence of elevated $[K^+]_o$, except for a slight attenuation at 75 mM $[K^+]_o$. In contrast, the inhibition of the currents by BB FCF, a more specific Panx1 inhibitor[25], was attenuated in a $[K^+]_o$ dose-dependent manner (Figure 3). Considering, that the putative binding sites for ATP and BB FCF overlap[25], it seems plausible that the putative binding sites of K^+ and BzATP on Panx1 channels overlap as well. However, it cannot be excluded that K^+ affects the ATP binding site allosterically.

Panx1 activation, a path to cell death? The Panx1 membrane protein exhibits a long stretch of amino acids at the carboxyterminus that is located at the cytoplasmic surface of the plasma membrane. Truncation of carboxy-terminal sequences was typically tolerated, basic channel functions remained preserved, as observed for Panx1 359stop or Panx1 408stop, for example. When expressed in oocytes, both mutants yielded currents similar in amplitude as wtPanx1 and sensitivity to Panx1 inhibitors, such as carbenoxolone, was preserved (Figure 4a). Only when Panx1 was truncated at position 378 to mimic cleavage of the protein by caspase-3[27] were the gating properties altered. The channel became constitutively active and the rectification prominently seen with wtPanx1 was absent (Figure 4b). As a consequence, the cells expressing this truncation mutant died when incubated for >12 hours. Although the Panx1 inhibitors carbenoxolone (CBX) or Probenecid efficiently inhibited currents mediated by Panx1

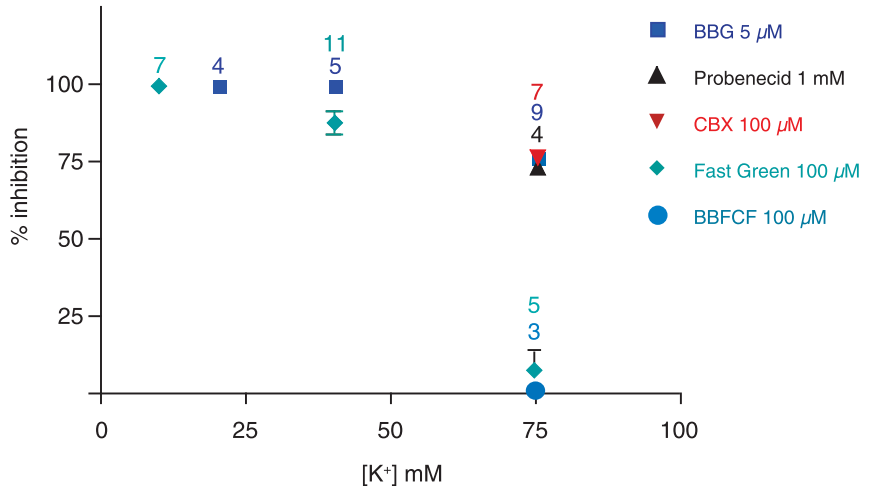

Figure 3 | Inhibition of K^+-induced currents by different Panx1 inhibitors as a function of $[K^+]_o$. With the exception of BB FCF and Fast green FCF, inhibition of Panx1 currents was independent of the $[K^+]_o$. Only at 75 mM $[K^+]$, a slight attenuation was observed. The inhibition by BB FCF and Fast Green FCF was attenuated at 40 mM and not detectable at 75 mM $[K^+]$.

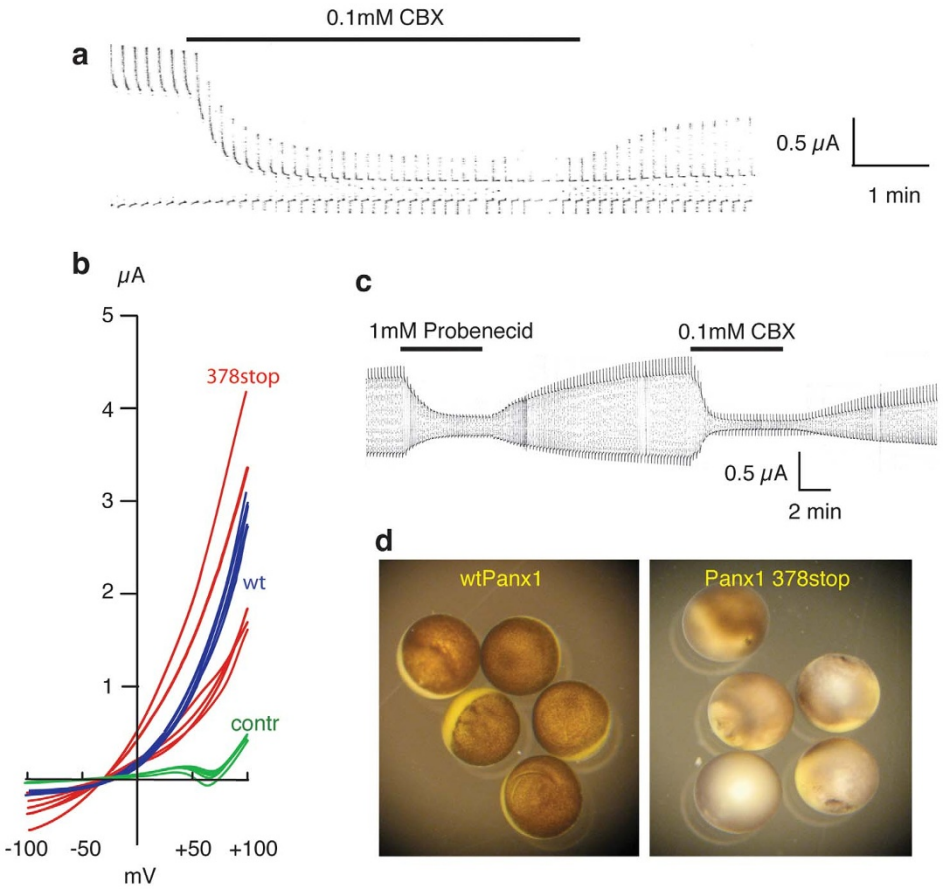

Figure 4 | Pannexin truncation and cell survival. The truncation mutants Panx1 359stop and Panx1 408stop form channels similar to wtPanx1. (a) Oocytes expressing Panx1 408stop were voltage clamped, held at -50 mV and stepped to +50 mV at a rate of 0.1 Hz. The voltage steps induced large currents that were sensitive to the Panx1 inhibitor carbenoxolone (CBX). The truncation mutant Panx1 378stop forms a constitutively open channel. (b) Voltage ramps from −100 to +100 mV were applied to uninjected oocytes (green, control) and oocytes expressing wtPanx1 (blue) or Panx1 378stop (red). Recordings were taken 48 hours after mRNA injection of wt Panx1 or 9 hours after injection of Panx1 378stop. Survival of Panx1 378stop expressing cells was limited and thus did not allow for longer incubation times, hence some currents with smaller amplitude than wtPanx1. The rectification typical for wtPanx1 was absent for Panx1 378stop. Furthermore, the reversal potential was shifted to the left for the mutant. (c) The Panx1 inhibitors probenecid and carbenoxolone (CBX) reversibly inhibited currents through Panx1 378stop channels. (d) Oocytes expressing wtPanx1 were viable 48 hours after mRNA injection (left), while oocytes expressing Panx1 378stop had undergone cell death already 36 hours after mRNA injection despite of incubation in Ringer's solution supplemented with 100 μM CBX.

378stop (Figure 4c), the cells died even when incubated with these Panx1 inhibitors (Figure 4d). This finding is in contrast to the mutants Panx1 C40S and Panx1 C346S that also are constitutively active, but the cells expressing them survive when incubated in CBX containing medium[28,29].

Panx1 mediates astrocyte cell death. To provide further evidence for the participation of Panx1 in mediating cell death, we measured LDH release from wild-type (WT), Panx1 knockout (KO) and $P2X_7R$ KO astrocytes exposed to 50 mM $[K^+]_o$. As indicated in Figure 5A, the two-fold increase in LDH release recorded from WT cells was abrogated by blocking Panx1 channels with MFQ (100 nM), in cells lacking Panx1 but not in cells lacking the $P2X_7R$ (Figure 5A).

To test whether BzATP attenuates LDH release, as predicted from the oocyte expression data described above, we stimulated WT astrocytes for 2 hr with elevated $[K^+]_o$ ACSF and determined the release of LDH in the absence and presence of BzATP (30 and 300 μM). As shown in Figure 5B, 25 mM $[K^+]_o$ elicited a significant loss of LDH from the astrocytes that was prevented only when the higher BzATP concentration was used. Interestingly, the addition of 30 μM BzATP boosted LDH release, probably by stimulating $P2X_7R$ without inhibiting Panx1.

Panx1-dependent caspase-3 activation. Apoptotic cell death involves the sequential activation of caspases, mainly caspase-3, a death protease that cleaves over 50 substrates, including Panx1[27,30]. Based on our finding that activation of Panx1 by elevated extracellular $[K^+]$ induces astrocyte cell death (Figure 5), we evaluated whether caspase-3 was involved in this process. Exposure of WT astrocytes for 1–2 hrs to elevated $[K^+]_o$ solution led to caspase-3 activation, as seen by the nuclear localization of a fluorescent cleaved caspase-3 substrate, DEVD (Figure 6A). The fraction of cells exhibiting nuclear DEVD staining was not significantly different if astrocytes were exposed to 10, 25 or 50 mM extracellular $[K^+]$ (Figure 6B), suggesting that maximal threshold for caspase-3 activation is obtained even with the lowest $[K^+]_o$ used. Elevated extracellular $[K^+]$ (25 and 50 mM) also led to caspase-3 activation in $P2X_7R$ KO but not in Panx1 KO astrocytes (Figure 6B), indicating that under these conditions, Panx1 expression is necessary and sufficient for the triggering of caspase-3 cleavage.

Next, we evaluated the extent to which BzATP could overcome Panx1-induced caspase-3 activation by elevated $[K^+]_o$. At 10 mM, K^+-induced activation of caspase-3 in WT astrocytes was prevented by 30 and 300 μM BzATP (Figure 6C); however, increasing $[K^+]_o$ to 50 mM reverted the agonist induced blocking effect (Figure 6C). Similar to the effects recorded in WT astrocytes, BzATP did not

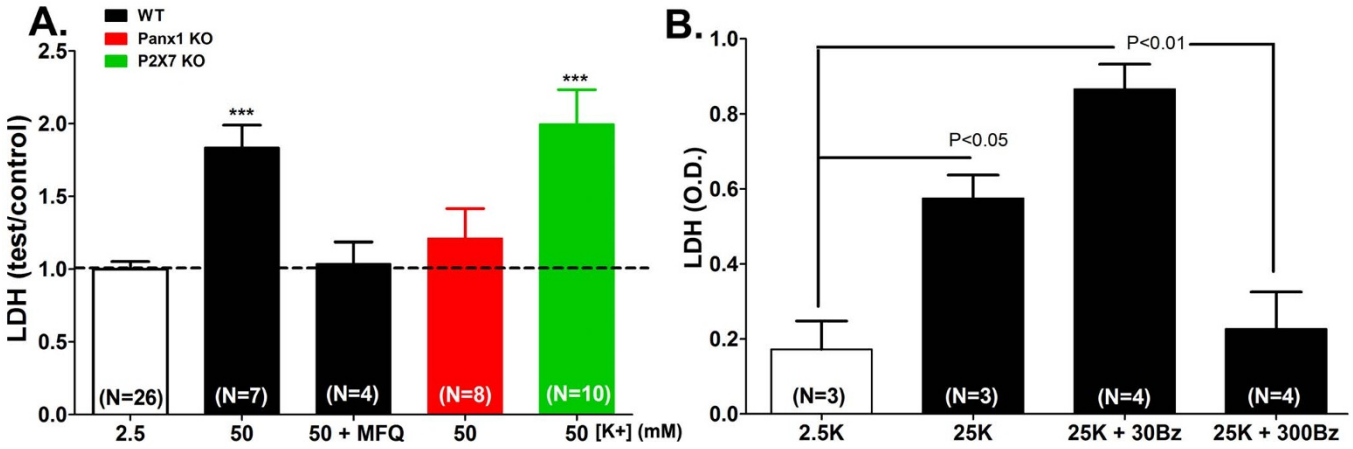

Figure 5 | Panx1 mediates astrocyte cell death. (A) Means ± s.e.m. values of fold changes in LDH released from WT (black), Panx1 KO (red) and $P2X_7R$ KO (green) astrocytes exposed for 1 hr to 50 mM K^+-ACSF relative to control condition (2.5 mM K^+ ACSF; white bar). Note that mefloquine (MFQ) at 100 nM blocked LDH released from WT cells. (B) LDH released from astrocytes exposed for 1 hr to 25 mM K^+-ACSF is enhanced by 30 μM BzATP and blocked by 300 μM BzATP. ***$P < 0.001$ (ANOVA followed by Tukey multiple comparison test). In parentheses are the number of samples.

prevent caspase-3 activation in $P2X_7$ KO cells exposed to 50 mM $[K^+]_o$ (Figure 6C). In Panx1 KO astrocytes, as expected, elevated $[K^+]_o$ or BzATP addition did not alter the fraction of nuclear DVEV positive cells compared to control (2.5 mM $[K^+]_o$) conditions (Figure 6C). That the effects of K^+ and BzATP on caspase-3 activation is mediated by Panx1 is further supported by experiments showing that 5 μM BBG and 100 μM fast green FCF, two compounds that inhibit Panx1 channels[16,25] attenuated K^+-induced caspase-3 activation in WT astrocytes and were innocuous on Panx1 KO cells (Figure 6D). Thus, these results provide strong evidence for the contribution of Panx1 to caspase-3 activation and that the combination of the two stimuli (elevated $[K^+]_o$ and ATP) is deleterious to astrocytes.

The redistribution of membrane phosphatidylserine (PS) from the inner to the outer leaflet of the plasma membrane is common to many apoptotic cells. To investigate whether Panx1 activation induced PS surface expression, WT and Panx1 KO astrocytes were treated with 10 mM K^+-ACSF (in the absence and presence of 300 μM BzATP) for 1 h and stained with annexin V-Texas red. As shown in Figure 7, high K^+-ACSF resulted in a slight, but not significant ($P > 0.05$ ANOVA), increase in annexin V staining in WT astrocytes that was prevented by exposing the cells to high K^+-ACSF

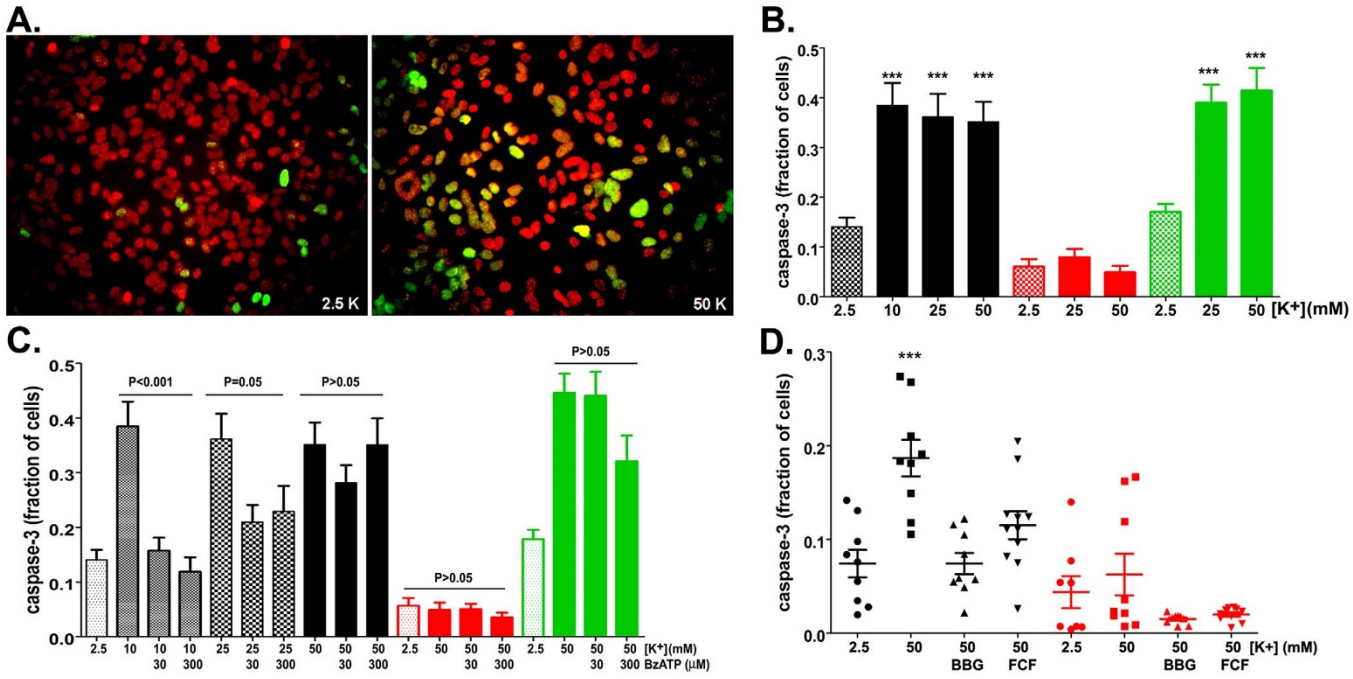

Figure 6 | Panx1-dependent caspase-3 activation. (A) Representative epifluorescence image showing cleaved caspase-3 (green) in nuclei (red) of WT astrocytes exposed to ACSF containing 2.5 and 50 mM $[K^+]$. (B) Histograms of the mean ± s.e.m values of the fraction of WT (black bars), Panx1 KO (red bars) and $P2X_7$ KO (green) astrocytes displaying cleaved caspase-3 following exposure to 10, 25 and 50 mM K^+-ACSF. ***$P < 0.001$ (ANOVA followed by Tukey multiple comparison test. Minimum of 4 independent experiments). (C) Bar histograms of the mean ± s.e.m. values of caspase-3 positive cells (relative to control) exposed to elevated extracellular $[K^+]$ in the absence and presence of BzATP. (D) Effect of BBG (5 μM) and BB FCF (100 μM) on caspase-3 activation induced by 50mM K^+-ACSF in WT (black symbols) and Panx1 KO (red symbols). Note that in Panx1 KO astrocytes high $[K^+]$ did not lead to caspase-3 activation. ***$P<0.001$ (ANOVA followed by Tukey' multiple comparison test). Mean+ s.e.m. are from 9–11 fields obtained from 3–4 different cultures.

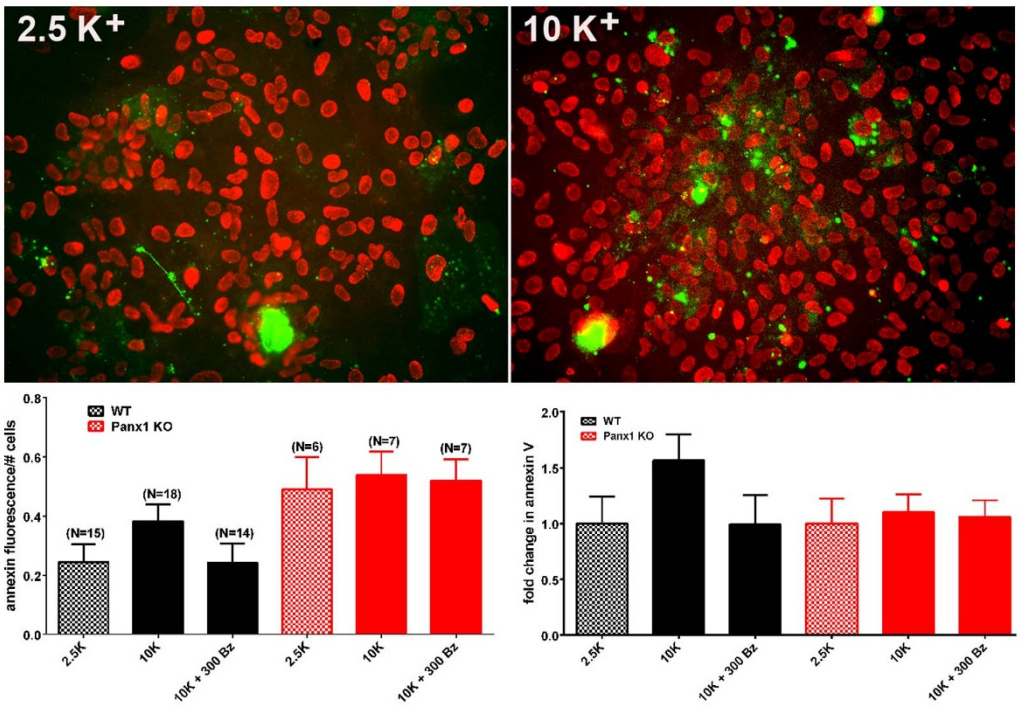

Figure 7 | AnnexinV staining in astrocytes. (Top) Examples of epifluorescence images of cultured WT astrocytes treated for 1–2 hr with 2.5 and 10 mM K^+- ACSF showing staining for Annexin V (green) and Dapi (red). (Bottom) Mean ± s.e.m. values of Annexin V fluorescence per total number of nuclei (left) and the mean ± s.e.m. fold changes in Annexin V (right) obtained for WT and Panx1 KO exposed to 2.5 mM K^+-ACSF and to 10 mM K^+-ACSF in the absence and presence of 300 μM BzATP. In parentheses are the number of images used for measurements that were obtained from 2 Panx1KO and 3 WT mice. Note that although not significant, there was a slight increase in Annexin V as measured in WT astrocytes exposed to 10 mM K^+-ACSF. To avoid any bias, we measured total fluorescence and divided by cell number. This procedure results in an underestimation of K+-induced cell death because of a few dead cells in the control condition that were highly fluorescent.

containing 300 μM BzATP. No changes in annexin V staining were recorded in Panx1 KO astrocytes submitted to similar conditions (Figure 7). These data suggested a minor contribution of Panx1 activation to PS externalization. It should, however, be noted that the analysis procedure used here results in an underestimation of the effect.

$P2X_7R$ agonist blocks Panx1 channels in neurons and astrocytes. To test whether the observations made in an expression system and cell cultures would also apply to an *in situ* condition, we used brain slices prepared from WT, Panx1 KO, $P2X_7R$ KO and double (d) Panx1 and $P2X_7R$ KO mice. Previously we have shown that in hippocampal slices elevation of extracellular K^+ induces influx of the dye YoPro1 in neurons and astrocytes in a Panx1 dependent manner[31]. Using the same *in situ* approach to measure Panx1 activity, we here show that BzATP blocks YoPro1 uptake induced by elevated $[K^+]_o$ (Figure 8). The 1.31 ± 0.04 and 1.11 ± 0.02 (N = 11 slices) fold increase in YoPro fluorescence recorded respectively from strata pyramidale and radiatum of the hippocampus of WT mice exposed to 50 mM K^+ ACSF were completely blocked by 300 μM BzATP (black symbols in Figure 8). Similar to WT, BzATP prevented the 1.15 ± 0.04 and 1.07 ± 0.02 (N = 9 slices) fold increase in YoPro uptake in the strata pyramidale and radiatum of hippocampus of $P2X_7R$ KO exposed to high K^+-ACSF (green symbols in Figure 8). No significant dye uptake was measured from hippocampal slices of Panx1 KO and of the dKO mice exposed to 50 mM K^+ ACFS, in the presence or absence of BzATP (Figure 8: red and yellow symbols, respectively). These data provide further support for the involvement of Panx1 in dye uptake and confirm that agonists of the $P2X_7$ receptors are indeed blockers of Panx1 channels.

Discussion

The biochemical and ionic changes resultant from the death of compromised cells within areas of hemorrhage, edema, or ischemia lead to the bystander damage (necrosis or apoptosis) of nearby cells. This secondary injury is regarded as being more destructive than the initial insult and thus is mainly responsible for functional deficits in the CNS. Elevation of the extracellular concentrations of excitatory neurotransmitters (e.g., glutamate, aspartate, ATP) and ions (mainly K^+) resultant from the initial insult trigger the progressive and long lasting secondary wave of cell death. As a consequence of ionic derangement, calcium influx into neural cells activates caspase and phospholipase pathways involved in necrosis and apoptosis[32]. Activation of P2 receptors by elevated ATP is one of the initial signals leading to inflammatory responses and pyroptotic cell killing[1–4].

Here we provide evidence that Pannexin1 is a key molecule that orchestrates caspase-dependent cell death in response to elevation of extracellular K^+ and ATP concentrations. Athough we have restricted our investigation to the combined effects of ATP and $[K^+]_o$ on Panx1 channels, it is clear that other molecules are also involved in Panx1-mediated cell death. For instance, glutamate released from damaged cells stimulates Panx1 through the NMDA receptors (Thompson et al., 2006), and the low oxygen environment resulting from obstructed/severed blood vessels and from edema is a known condition that activates Panx1 channels[19,21,22].

Panx1 forms plasma membrane channels that are activated directly by K^+ ([7]) and, through intracellular signaling cascades, by ATP-sensitive P2 receptors[33,34]. Activation of Pannexin1 by elevated extracellular $[K^+]$ has been reported to induce caspase-1 activation and IL-1β release[7] and to release ATP[11,15,21,35]. The potentially deleterious consequences of ATP-mediated cell death by hyperactivation of the innate immune response via such a Panx1 positive feedback

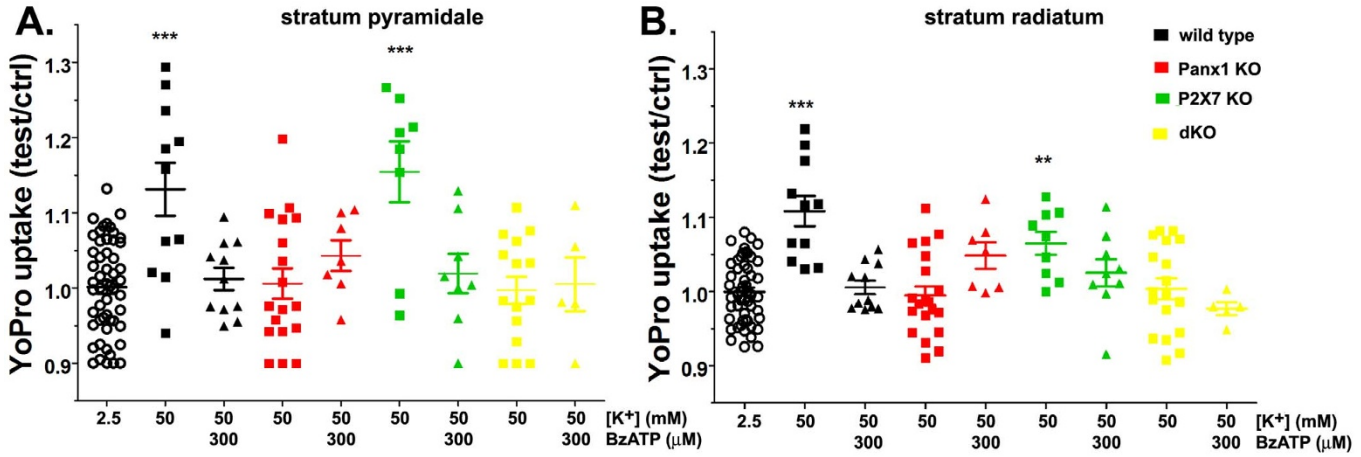

Figure 8 | *In situ* blockade of Panx1 channels by BzATP. Means ± s.e.m. of the relative values (test/control) of YoPro fluorescence changes induced by 50 mM K^+-ACSF in the absence and presence of 300 μM BzATP recorded from strata pyramidale (left) and radiatum (right) of hippocampi of wild-type (black symbols), Panx1 KO (red symbols), $P2X_7R$ KO (green symbols) and dKO (yellow symbols) mice. Data for each genotype were normalized to their corresponding values recorded at 2.5 mM K^+-ACSF (open circles). ***$P < 0.001$, **$P < 0.01$ (ANOVA followed by Dunnet's test). Each symbol correspond to values obtained from a single hippocampal slice from a minimum of three mice per genotype.

loop (ATP-induced ATP release) is counteracted by the inhibitory action of ATP on Panx1 itself[16]. This is illustrated in a model (Figure 9) where a control loop occurs in the simplest form, the permeant (ATP) inhibits its own release channel. Since, the affinity of ATP to P2 receptors is higher than that to Panx1, a controlled signaling event mediated by low $[ATP]_o$ can spread from cell to cell without threatening cell integrity. Indeed, calcium waves in endothelial cell layers, airway epithelium and astrocytes appear to operate by ATP released through Panx1 channels acting on purinergic receptors which in turn activate Panx1 channels in adjacent cells[11,21,35,36]. However, at high $[ATP]_o$, as occurring in the vicinity of dying cells, ATP blockade of Panx1 channels will ensue.

The present study demonstrates that the negative feedback control of ATP on Panx1 channels can be abrogated when the extracellular K^+ concentration is elevated. Thus, even minimal activation of the purinergic receptor by modest increases in extracellular ATP may lead to an unopposed positive feedback loop, that eventually could hyperactivate the purinergic receptor and associated downstream events. The lack of the negative feedback control could, therefore, be a major contributing factor to cell death by ATP in an environment with increased extracellular K^+ concentration. Indeed, our results show that $[K^+]_o$ above 10 mM is sufficient to attenuate the inhibitory action of ATP/BzATP on oocyte Panx1 currents.

The extracellular K^+ concentrations ($[K^+]_o$) found here to attenuate the inhibitory effect of ATP on Panx1 channels are high and typically do not occur in the extracellular space except in the inner ear or in Pacinian corpuscles, for example. In normal CNS, the $[K^+]_o$ is low and undergoes minor variations in response to neuronal activity[10]. However, it has been determined, that after middle cerebral artery occlusion, $[K^+]_o$ in the infarct core increased to >50 mM, progressively decreasing in the penumbra[8,9]. Similarly, high $[K^+]_o$ has been observed during spreading depression in the cerebral cortex[10]. A more moderate increase of $[K^+]_o$ to circa 10 mM has been observed during epileptiform convulsions[10]. Thus, under pathological conditions, the scenario for attenuation of the auto-inhibition of Panx1 channels by ATP can exist.

Traumatic brain injury and stroke induce innate immune responses characterized by activation of the inflammasome, a multiprotein complex that is regulated by XIAP, $P2X_7$ receptors, and Panx1 (reviewed in[37]). During these acute injuries to the CNS, the loss of ATP-induced inhibition of Panx1 channels in such a potassium-rich environment could be a key factor for hyperstimulation of the inflammasome in neighboring healthy cells resulting in immunogenic cell death. In this scenario, the signaling chain *purinergic receptor stimulation > Panx1 activation > ATP release > purinergic receptor activation* might be sufficient for cell death due to the hyperactivation of the inflammasome and loss of the barrier function of the membrane.

In addition to the involvement of Panx1 in caspase-1 activation and pyroptotic cell death[7], our results show that Panx1 is upstream in the caspase-3 signaling cascade involved in apoptotic cell death. In support to an early role of Panx1 in apoptotic cell death is our data showing that activation of caspase-3 is inhibited by Panx1 inhibitors and prevented in astrocytes lacking Panx1. These findings, however, do not contradict a previous report showing that caspase-3 activation renders the Panx1 channel constitutively open[27]. We found that a truncated Panx1 (378 stop) mimicking the caspase-3 cleaved protein also rendered the channel constitutively active and induced oocyte cell death. However, further truncation (359stop or 408stop) yielded "normally" gated channels, indicating that a precise cleavage rather than removing a carboxy-terminal plug is responsible for the altered gating of the Panx1 channel. Thus, it seems that Panx1 exerts a role upstream of caspase-3 in addition to the downstream role, where caspase-3 "further" activates the Panx1 channel irreversibly after cells commit to apoptotic/pyroptotic death[27].

Data obtained from a study using Panx1-deficient mice have been interpreted as Panx1 not being required for activation of the inflammasome[38]. The experimental evidence for this conclusion was based on the response of macrophages to high extracellular ATP concentrations (3–5 mM). At this extreme concentration of ATP, activation of the $P2X_7R$-inflammsasome axis certainly would not benefit from any amplification by the ATP release function of Panx1. Thus, there is no contradiction between the Qu et al. study[38] and the data presented in the present study as to whether Panx1 is required for pyroptotic cell death under any experimental conditions. The present data, however, suggest that in the presence of Panx1, the threshold for cells to undergo apoptosis is considerably lower when stimuli of the apoptotic pathway synergize.

The data presented here also have consequences for the usefulness of Panx1 inhibitors as therapeutic agents. Increased extracellular $[K^+]$ not only attenuated the self-inhibition of Panx1 but also affected other Panx1 channel inhibitors, notably the inhibition of the Panx1 channel by BB FCF. Considering that ATP and BB FCF involve overlapping amino acid sequences to exert their effect on Panx1 channels this is not surprising. The less specific Panx1 inhibitors, carbenoxolone and Probenecid, were still inhibitory in the

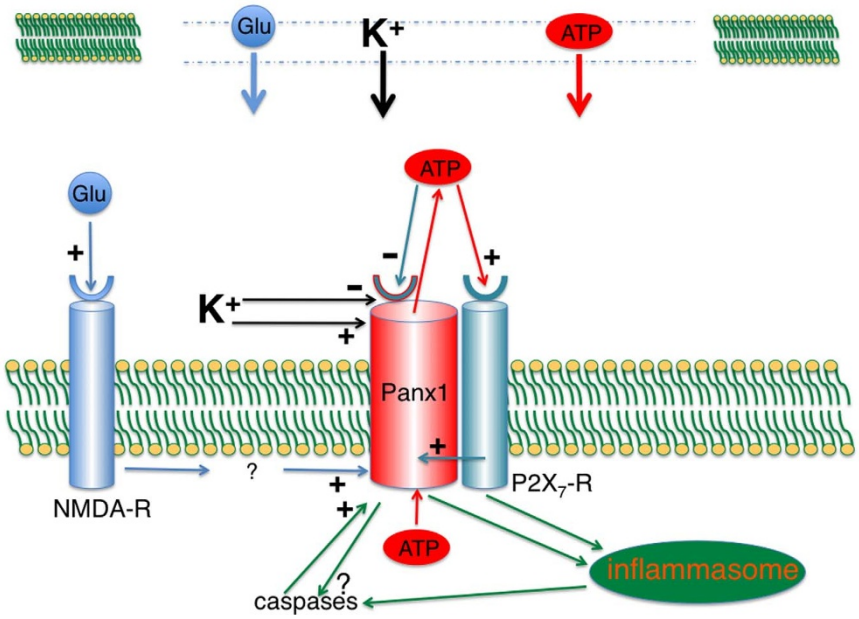

Figure 9 | Early signaling events in cell undergoing secondary cell death. In the central nervous system, damaged cells (top) release ATP, glutamate and K^+ into a narrow extracellular space and thus can reach concentrations approximating those in the cytoplasm. Extracellular ATP binds to purinergic receptors, including $P2X_7R$, activating it and also activating the Panx1 channel through intracellular signaling cascade[33,34]. ATP efflux through the Panx1 channel[15] then provides a positive feedback for $P2X_7R$ activation. Under normal circumstances this positive feedback would be interrupted by the inhibition of the Panx1 channel by extracellular ATP[16,18,41]. Increased $[K^+]_o$ renders this negative feedback loop ineffective as shown in the present study. In addition, $[K^+]_o$ stimulates Panx1 directly[7]. $P2X_7R$ and/or Panx1 signal to the inflammasome and thereby activate caspase-1[7,12]. In addition, caspase-3 gets activated through an unknown pathway (present study). Panx1 is a substrate of caspase-3 and its cleavage results irreversibly in constitutive channel activity[27]. Cell death thus is a combination of apoptotic events combined with the rundown of all membrane gradients for small molecules due to the permanently active Panx1 channel.

presence of elevated $[K^+]$. The attenuation of the inhibitory effect of BB FCF on Panx1 currents was only prominent at very high $[K^+]_o$ (75 mM). Thus, in some pathological conditions, BB FCF may still be useful to curb deleterious effects of excessive Panx1 channel activity.

In summary, the present results demonstrate that the negative feedback control of ATP release through Panx1 channels can be abrogated when the extracellular K^+ concentration is elevated. This situation is given in the vicinity of dying or dead cells as in CNS injuries. Both molecules activate Panx1 in adjacent healthy cells, indirectly through purinergic receptors and in the case of K^+, acting directly on the channel. Activation of Panx1 channels then leads to caspase-dependent cell death by activating the inflammasome and caspases through $P2X_7R$ and maybe even directly. We propose that any ATP release mechanism associated with and activated by purinergic receptors needs an inhibitory mechanism to insure a measured response of a cell to an ATP signal. Otherwise, a positive feedback loop could rapidly deplete the cell of ATP and, more seriously, induce ATP-mediated cell death. To our knowledge, Panx1 is the only ATP release channel where such a negative feedback control has been identified[16].

Methods

All experiments involving cells derived from animals were performed in accordance with the approved guidelines and sanctioned by animal protocols at the University of Miami and Albert Einstein College of Medicine.

Preparation of oocytes. Preparation of oocytes and electrophysiological recording were performed as described previously[39,40].

Synthesis of mRNA. Panx1, in pCS2, was linearized with NotI, In vitro transcription was performed with the polymerase SP6, using the Message Machine kit (Ambion). mRNA was quantified by absorbance (260 nm), and the proportion of full length transcripts was checked by agarose gel electrophoresis. In vitro–transcribed mRNA (~20 nl) was injected into *Xenopus laevis* oocytes. Site-directed mutations were generated according to the protocol of the QuikChange II Site-Directed Mutagenesis kit (Agilent Technologies).

Electrophysiology. Whole cell membrane current of single oocytes was measured using a two-electrode voltage clamp and recorded with a chart recorder. Both voltage-measuring and current-passing microelectrodes were pulled with a horizontal puller (Sutter Instruments Co) and filled with 3 M KCl. The recording chamber was perfused continuously with frog Ringer (OR2) solution (mM: 82.5 NaCl, 2.5 KCl, 1 $CaCl_2$, 1 $MgCl_2$, 1 Na_2HPO_4, and 5 HEPES, pH 7.5). Membrane conductance was determined using voltage pulses. Oocytes expressing Panx1were held at −60 mV, and pulses to +60 mV were applied to transiently open the channels by means of the voltage gate. For activation by K^+, the membrane potential was held at −50 mV and 10 mV voltage steps were applied at 0.1 Hz for conductance measurements. Voltage ramps were applied with a custom-made device and the ramps lasted 70 seconds.

Mice. The Panx1-null mouse line ($Panx1^{tm1a(KOMP)Wtsi}$), generated by KOMP (www.KOMP.org) in the C57Bl6 background and the $P2X_7R^{-/-}$ mice (*P2rx7*^{tm1Gab}/J) in the C57Bl6 background purchased from Jackson laboratories were maintained in our animal facility at Albert Einstein College of Medicine. Crossing Panx1-null with $P2X_7^{-/-}$ mice were used to generate double Panx1:$P2X_7$-null mice that were maintained in our animal facility. All studies were performed following protocols approved by the Albert Einstein Animal Care and Use Committee.

Hippocampal Slices. Slices were prepared as previously described[31]. Briefly, coronal sections (350 μm thick) of P13–P14 mouse brains were obtained using a tissue chopper (Ted Pella Inc.). After cutting, brain slices were immediately placed in Hepes buffered, air-bubbled ACSF (145 mM NaCl, 2.5 mM KCl, 3.1 mM $CaCl_2$, 1.3 mM $MgCl_2$, 10 mM glucose, 10 mM Hepes, pH 7.4), and maintained at 30°C. After 30–40 min, ACSF was exchanged for the appropriate ACSF necessary for each experimental condition (see below).

YoPro uptake. Panx1 activation was evaluated in acute hippocampal slices using a method of dye uptake, previously described[31]. Briefly, brain slices were incubated for 1 hr, at 30°C, in HEPES-buffered air-bubbled ACSF (normal and high $[K^+]_o$) containing the dye (5 μM), in the absence and presence of Benzoyl-benzoyl-adenosine triphosphate (BzATP: 300 uM; Sigma). After that, YoPro solution was removed and slices washed 3 times, 10 min each with 5 ml ACSF. After the last wash, brain slices were fixed overnight, at 4°C, in 4% p-formaldehide, and then transferred to ice-cold ACSF containing 30% sucrose for few hours and hippocampal slices isolated from the surrounding brain tissue. YoPro1 uptake in hippocampi following exposure to ACSF containing 2.5 mM and 50 mM $[K^+]_o$ concentrations (osmolarity adjusted with equimolar concentration of NaCl) was measured from regions of interest placed on the stratum pyramidale (CA1–CA3) and stratum radiatum of p-

formaldehyde fixed tissues using an Nikon inverted microscope equipped with 4× objective, 488/512 nm filter sets and Metafluor software.

Astrocyte culture. Cultures were prepared as described previously[11]. Brain cortices of neonatal (P0–P1) mice were minced in ice cold Ca^{2+}-free Dulbecco's phosphate buffered saline (DPBS, Cellgro, Herndon, VA) and tissue digested with 0.05% trypsin (Cellgro) for 5 min at 37°C, after which digests were centrifuged at 1.500 RPM for 5 min. Supernatants were removed and cells re-suspended in Dulbecco's minimal essential medium (DMEM, Invitrogen, NY, USA) containing 10% fetal bovine serum (FBS, Invitrogen) and 1% penicillin/streptomycin antibiotics (Invitrogen). Cells were grown for 1–2 weeks in plastic tissue cultures dishes (BD Falcon, NJ, USA) and maintained at 37°C in a humidified 5% CO_2 incubator.

Caspase-3 activation and annexin V staining. The DEVD-NucView™ 488 caspase-3 substrate assay (Biotium) was used in experiment to evaluate caspase-3 activation in astrocytes, according to manufacture. Briefly, cultured astrocytes plated in glass bottomed dishes (MatTech) were washed with artificial cerebrospinal fluid (ACSF) and incubated for 1–2 hrs in high K^+ ACSF containing 5 μM fluorogenic caspase-3 substrate at RT. In some experiments Texas red conjugated (CF^{594})-Annexin V (1 μM; Biotium) was added to the solution. After 3 washes in control ACSF, cells were fixed with 4% p-formaldehyde for 5 min prior to the addition of mounting medium (Vectashild) containing the nuclear marker DAPI. Epifluorescent images were capture with Metafluor software using a CoolSNAP-HQ2 CCD camera (Photometrics, AZ, USA) attached to an inverted microscope (Eclipse TE-2000 Nikon) equipped with 20× dry objective and 346, 488 and 594 nm filter sets. Analyses were performed by counting the number of nuclei stained with DEVD relative to those stained with DAPI using a subroutine of Image-J software that allows quantitation of number of particles in binary images. For Annexin V quantification, mean CF^{594}-Annexin fluorescence intensity in a field of view was divided by the number of nuclei using Image-J software.

LDH release. To quantify the release of lactate dehydrogenase (LDH) from astrocytes, the cytotoxicity detection kit (#04744926001, Roche Applied Science) was used according to manufacture instruction. Astrocyte cultures were exposed for 1 hr to control or high K^+ -ACSF containing or not MFQ (100 nM) or BzATP (30 and 300 μM). Samples (100 μl) of cell bathing solutions were transferred to a 96 well plate and incubated for 30 min at RT with the LDH reagents. After addition of the stop solution, generated formazan dye was quantified (absorbance at 490 nm) using a plate reader (BGM-LABTECH).

1. Zheng, L. M., Zychlinsky, A., Liu, C. C., Ojcius, D. M. & Young, J. D. Extracellular ATP as a trigger for apoptosis or programmed cell death. *J Cell Biol* **112**, 279–288 (1991).
2. Di Virgilio, F., Pizzo, P., Zanovello, P., Bronte, V. & Collavo, D. Extracellular ATP as a possible mediator of cell-mediated cytotoxicity. *Immunol Today* **11**, 274–277 (1990).
3. Ferrari, D. *et al.* ATP-mediated cytotoxicity in microglial cells. *Neuropharmacology* **36**, 1295–1301 (1997).
4. Burnstock, G. Purinergic signalling and disorders of the central nervous system. *Nat Rev Drug Discov* **7**, 575–590 (2008).
5. Qu, Y., Franchi, L., Nunez, G. & Dubyak, G. R. Nonclassical IL-1 beta secretion stimulated by P2X7 receptors is dependent on inflammasome activation and correlated with exosome release in murine macrophages. *J Immunol* **179**, 1913–1925 (2007).
6. de Rivero Vaccari, J. P. *et al.* P2X4 receptors influence inflammasome activation after spinal cord injury. *J Neurosci* **32**, 3058–3066 (2012).
7. Silverman, W. R. *et al.* The pannexin 1 channel activates the inflammasome in neurons and astrocytes. *J Biol Chem* **284**, 18143–18151 (2009).
8. Sick, T. J., Feng, Z. C. & Rosenthal, M. Spatial stability of extracellular potassium ion and blood flow distribution in rat cerebral cortex after permanent middle cerebral artery occlusion. *J Cereb Blood Flow Metab* **18**, 1114–1120 (1998).
9. Gido, G., Kristian, T. & Siesjo, B. K. Extracellular potassium in a neocortical core area after transient focal ischemia. *Stroke* **28**, 206–210 (1997).
10. Somjen, G. G. Extracellular potassium in the mammalian central nervous system. *Annu Rev Physiol* **41**, 159–177 (1979).
11. Suadicani, S. O. *et al.* ATP signaling is deficient in cultured pannexin1-null mouse astrocytes. *Glia* **60**, 1106–1116 (2012).
12. Gulbransen, B. D. *et al.* Activation of neuronal P2X7 receptor-pannexin-1 mediates death of enteric neurons during colitis. *Nat Med* **18**, 600–604 (2012).
13. Locovei, S., Wang, J. J. & Dahl, G. Activation of pannexin 1 channels by ATP through P2Y receptors and by cytoplasmic calcium. *FEBS Letters* **580**, 239–244 (2006).
14. Locovei, S., Scemes, E., Qiu, F., Spray, D. C. & Dahl, G. Pannexin1 is part of the pore forming unit of the P2X(7) receptor death complex. *FEBS Lett* **581**, 483–488 (2007).
15. Bao, L., Locovei, S. & Dahl, G. Pannexin membrane channels are mechanosensitive conduits for ATP. *FEBS Lett* **572**, 65–68 (2004).
16. Qiu, F. & Dahl, G. A permeant regulating its permeation pore: inhibition of pannexin 1 channels by ATP. *Am J Physiol Cell Physiol* **296**, C250–255 (2009).
17. Ma, W. H., Hui, H., Pelegrin, P. & Surprenant, A. Pharmacological Characterization of Pannexin-1 Currents Expressed in Mammalian Cells. *JPET* **328**, 409–418 (2009).
18. Qiu, F., Wang, J. & Dahl, G. Alanine substitution scanning of pannexin1 reveals amino acid residues mediating ATP sensitivity. *Purinergic Signal* **8**, 81–90 (2012).
19. Thompson, R. J., Zhou, N. & MacVicar, B. A. Ischemia opens neuronal gap junction hemichannels. *Science* **312**, 924–927 (2006).
20. Thompson, R. J. *et al.* Activation of pannexin-1 hemichannels augments aberrant bursting in the hippocampus. *Science* **322**, 1555–1559 (2008).
21. Locovei, S., Bao, L. & Dahl, G. Pannexin 1 in erythrocytes: Function without a gap. *Proc Natl Acad Sci U S A* **103**, 7655–7659 (2006).
22. Sridharan, M. *et al.* Pannexin 1 is the conduit for low oxygen tension-induced ATP release from human erythrocytes. *Am J Physiol Heart Circ Physiol* **299**, H1146–1152 (2010).
23. Silverman, W., Locovei, S. & Dahl, G. Probenecid, a gout remedy, inhibits pannexin 1 channels. *Am J Physiol Cell Physiol* **295**, C761–767 (2008).
24. Bruzzone, R., Barbe, M. T., Jakob, N. J. & Monyer, H. Pharmacological properties of homomeric and heteromeric pannexin hemichannels expressed in Xenopus oocytes. *J Neurochem* **92**, 1033–1043 (2005).
25. Wang, J., Jackson, D. G. & Dahl, G. The food dye FD&C Blue No. 1 is a selective inhibitor of the ATP release channel Panx1. *J Gen Physiol* **141**, 649–656 (2013).
26. Dahl, G., Qiu, F. & Wang, J. The bizarre pharmacology of the ATP release channel pannexin1. *Neuropharmacology* **75**, 583–593 (2013).
27. Chekeni, F. B. *et al.* Pannexin 1 channels mediate 'find-me' signal release and membrane permeability during apoptosis. *Nature* **467**, 863–867 (2010).
28. Wang, J. & Dahl, G. SCAM analysis of Panx1 suggests a peculiar pore structure. *J Gen Physiol* **136**, 515–527 (2010).
29. Bunse, S. *et al.* Single cysteines in the extracellular and transmembrane regions modulate pannexin 1 channel function. *J Membr Biol* **244**, 21–33 (2011).
30. Porter, A. G. & Janicke, R. U. Emerging roles of caspase-3 in apoptosis. *Cell Death Differ* **6**, 99–104 (1999).
31. Santiago, M. F. V. J., Patel, N. K., Lutz, S. E., Caille, D., Charollais, A., Meda, P. & Scemes, E. Targeting Pannexin1 improves seizure outcome. *Plos One* **6**, e25178 (2011).
32. Borgens, R. B. & Liu-Snyder, P. Understanding secondary injury. *Q Rev Biol* **87**, 89–127 (2012).
33. Locovei, S., Wang, J. & Dahl, G. Activation of pannexin 1 channels by ATP through P2Y receptors and by cytoplasmic calcium. *FEBS Lett* **580**, 239–244 (2006).
34. Iglesias, R. *et al.* P2X7 receptor-Pannexin1 complex: pharmacology and signaling. *Am J Physiol Cell Physiol* **295**, C752–760 (2008).
35. Ransford, G. A. *et al.* Pannexin 1 contributes to ATP release in airway epithelia. *Am J Respir Cell Mol Biol* **41**, 525–534 (2009).
36. Iglesias, R., Dahl, G., Qiu, F., Spray, D. C. & Scemes, E. Pannexin 1: the molecular substrate of astrocyte "hemichannels" *J Neurosci* **29**, 7092–7097 (2009).
37. Walsh, J. G., Muruve, D. A. & Power, C. Inflammasomes in the CNS. *Nat Rev Neurosci* (2014).
38. Qu, Y. *et al.* Pannexin-1 Is Required for ATP Release during Apoptosis but Not for Inflammasome Activation. *J Immunol* **186**, 6553–6561 (2011).
39. Dahl, G. The Xenopus oocyte cell-cell channel assay for functional analysis of gap junction proteins., in *Cell-cell interactions. A practical approach.* (eds. Stevenson, B., Gallin, W. & Paul, D.) 143–165 (IRL, Oxford; 1992).
40. Dahl, G. & Pfahnl, A. Mutagenesis to study channel structure. *Methods Mol Biol* **154**, 251–268 (2001).
41. Dahl, G. & Keane, R. W. Pannexin: From discovery to bedside in 11+/−4 years? *Brain Res* **1487**, 150–159 (2012).

Acknowledgments

We thank Naman K. Patel for animal care and astrocyte cell culture. Work reported here was supported by a grant from the Craig Nielsen Foundation. We also thank our home institutions for additional support.

Author contributions

G.D., E.S. and R.W.K. designed research; D.G.J., J.W.and E.S. performed research; E.S., D.G.J., J.W. and G.D. analyzed data; and G.D., E.S. and R.W.K. wrote the paper.

Additional information

Competing financial interests: The authors declare no competing financial interests.

How to cite this article: Jackson, D.G., Wang, J.J., Keane, R.W., Scemes, E. & Dahl, G. ATP and potassium ions: a deadly combination for astrocytes. *Sci. Rep.* **4**, 4576; DOI:10.1038/srep04576 (2014).